IUCrData

ISSN 2414-3146

1,2-Bis[di(benzofuran-2-yl)phosphanyl]ethane

Sebastian Ahrens, Anke Spannenberg, Matthias Beller and Kathrin Junge*

Leibniz-Institut für Katalyse e. V., Albert-Einstein-Str. 29a, 18059 Rostock, Germany. *Correspondence e-mail: Kathrin.Junge@catalysis.de

Received 17 October 2025
Accepted 20 October 2025

Edited by L. Van Meervelt, Katholieke Universiteit Leuven, Belgium

Keywords: crystal structure; bidentate ligand; benzofuran; phosphine.

CCDC reference: 2496508

Structural data: full structural data are available from iucrdata.iucr.org

The title compound, $C_{34}H_{24}O_4P_2$, consists of an ethylene-bridged diphosphine with benzofuran residues, where the P—C—C—P backbone exhibits an *anti*-conformation. The asymmetric unit contains one half molecule, which is completed by inversion symmetry.

3D view

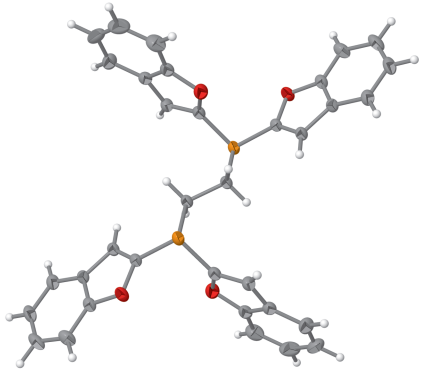

Chemical scheme

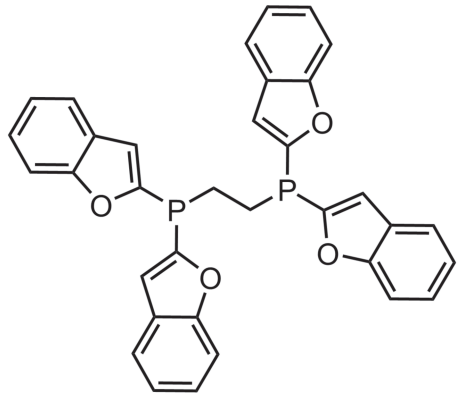

Structure description

Bidentate phosphine ligands play a pivotal role in homogeneous catalysis, where their chelation to a metal center enhances complex stability and allows precise control over electronic and steric properties (van Leeuwen *et al.*, 2000). Ethylene-bridged diphosphines, such as 1,2-bis(diphenylphosphanyl)ethane (dppe), are among the most widely used ligands owing to their versatile coordination behavior (Clevenger *et al.*, 2020). Variations in the substituents on phosphorus strongly influence catalytic activity, selectivity, and metal–ligand interactions. Consequently, structural modification of ethylene-bridged diphosphines remains a key strategy for the design of improved catalysts in transition-metal-mediated transformations. Numerous ethylene-bridged diphosphines have been synthesized, bearing alkyl substituents as well as aryl substituents (Dekker *et al.*, 1992).

Recently, our group demonstrated the potential of benzofuran-based phosphines in the Co-catalyzed isomerization of allylamines (Ahrens *et al.*, 2025). These studies revealed that benzofurylphosphines represent an alternative structural motif to conventional aryl phosphines, offering distinct electronic and steric properties that can significantly influence catalytic activity. Owing to their unique reactivity, structurally related phosphines have also been successfully applied in the Pd-catalyzed telomerization of butadiene (Souza *et al.*, 2025). In our previous work, only monodentate benzofuran phosphines were developed and evaluated in catalytic applications. To expand this ligand family, the corresponding bidentate analogue has now been synthesized. The new diphosphine 1,2-bis[di(benzofuran-2-yl)phosphanyl]ethane was prepared and its crystal structure determined.

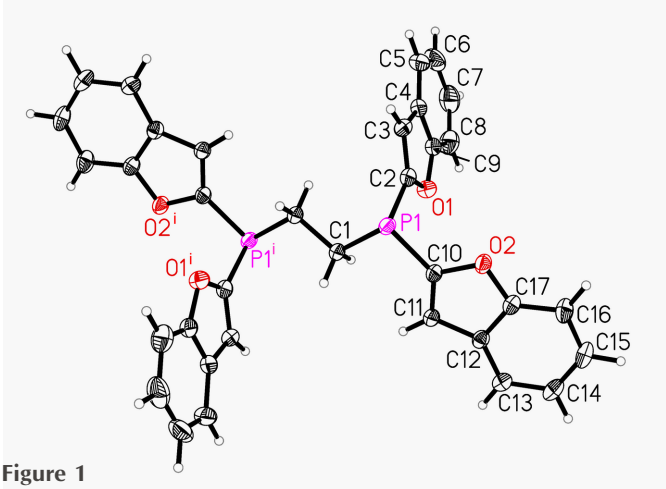

Figure 1
The molecular structure of the title compound with atom labeling and displacement ellipsoids drawn at 50% probability level [symmetry code: (i) $-x + 1, -y + 2, -z + 1$].

The molecular geometry of the title compound reflects the characteristic features of ethylene-bridged diphosphines with the P–C–C–P backbone forming a zigzag chain and exhibiting an *anti*-conformation (Fig. 1). Each phosphorus atom displays a pyramidal arrangement with two benzofuran substituents and one CH_2 group of the ethylene bridge. The P—C—C—P torsion angle amounts to 180°, bond lengths and angles are in the expected range. The dihedral angle between the benzofuran rings is 84.94 (3)°. The asymmetric unit contains one half-molecule expanded by the symmetry operation $-x + 1, -y + 2, -z + 1$.

Moreover, the electronic structure of the benzofuryl diphosphine differs significantly from that of dppe. In solution at room temperature, the ^{31}P NMR resonance is significantly upfield-shifted (–52.6 ppm compared to −12.6 ppm for dppe), indicating a higher electron density at the phosphorus atoms (Benny *et al.*, 2023). The increased shielding can be attributed to the greater π-donor strength and electron delocalization provided by the benzofuryl substituents. Therefore, the ligand shows an increased electron-donating character, altering the electron density and reactivity of its metal complexes relative to dppe.

Synthesis and crystallization

All synthetic procedures were carried out under argon atmosphere using standard Schlenk techniques. The anhydrous and oxygen-free solvents used (tetrahydrofuran, dichloromethane, diethyl ether, and *n*-pentane) were obtained from an Innovative Technology PS-MD-6 solvent purification system. The purified solvents were stored over 3 Å molecular sieves under argon. The reagents 1,2-bis(dichlorophosphanyl) ethane and benzofuran were obtained from Sigma-Aldrich and Fisher Scientific, respectively, and used as received.

NMR spectra were recorded on a Bruker Avance 300 spectrometer operating at 300 MHz for ^{1}H, 75 MHz for ^{13}C, and 121 MHz for ^{31}P. All chemical shifts (δ) are reported in ppm relative to tetramethylsilane (TMS). Solvent references for CD_2Cl_2 are δ = 5.32 ppm for ^{1}H and 53.84 ppm for ^{13}C. ^{31}P chemical shifts are reported relative to an external 85% H_3PO_4 standard.

Table 1
Experimental details.

Crystal data	
Chemical formula	$C_{34}H_{24}O_4P_2$
M_r	558.47
Crystal system, space group	Monoclinic, $P2_1/n$
Temperature (K)	150
a, b, c (Å)	5.6351 (5), 10.5372 (9), 22.7988 (19)
β (°)	93.696 (1)
V (Å^3)	1350.9 (2)
Z	2
Radiation type	Mo $K\alpha$
μ (mm^{-1})	0.20
Crystal size (mm)	0.35 × 0.17 × 0.11
Data collection	
Diffractometer	Bruker APEXII CCD
Absorption correction	Multi-scan (*SADABS*; Krause et al., 2015)
T_{min}, T_{max}	0.93, 0.98
No. of measured, independent and observed [$I > 2\sigma(I)$] reflections	23407, 3594, 3145
R_{int}	0.025
(sin $\theta/\lambda)_{max}$ (Å^{-1})	0.682
Refinement	
$R[F^2 > 2\sigma(F^2)]$, $wR(F^2)$, S	0.038, 0.102, 1.04
No. of reflections	3594
No. of parameters	181
H-atom treatment	H-atom parameters constrained
$\Delta\rho_{max}$, $\Delta\rho_{min}$ (e Å^{-3})	0.41, −0.28

Computer programs: *APEX2* (Bruker, 2014, *SAINT* (Bruker, 2013), *SHELXT* (Sheldrick, 2015*a*), *SHELXL* (Sheldrick, 2015*b*), *XP* in *SHELXTL* (Sheldrick, 2008) and *publCIF* (Westrip, 2010).

The synthesis of the title compound was carried out following literature procedures for ethylene-bridged diphosphines with minor modifications (Casey *et al.*, 1983). Under an argon atmosphere, anhydrous benzofuran (1.181 g, 10.0 mmol, 4 eq.) was charged in a Schlenk flask and dissolved in 20 ml of anhydrous THF. The solution was cooled to 253 K, and *n*-BuLi (2.5 *M*, 4.0 ml, 10.0 mmol, 4 eq.) was added dropwise. The reaction mixture was stirred for 2 h. Subsequently, 1,2-bis(dichlorophosphanyl)ethane (580 mg, 2.5 mmol, 1 eq.) was added slowly to the lithiated benzofuran solution. The reaction temperature was maintained at 253 K for 2 h before allowing the reaction mixture to warm to room temperature. After stirring overnight, the solvent was removed *in vacuo*, yielding a yellow solid. To remove lithium chloride, the yellow solid was dissolved in 60 ml of anhydrous diethyl ether and the resulting suspension was filtered under an inert atmosphere. 1,2-Bis[di(benzofuran-2-yl)phosphanyl] ethane was crystallized from a concentrated dichloromethane solution at 278 K to afford colorless, needle-shaped crystals (894 mg, 1.6 mmol, 64%). Crystals suitable for single-crystal X-ray diffraction were obtained by diffusion of *n*-pentane into a dichloromethane solution of the phosphine.

^{1}H NMR (300 MHz, CD_2Cl_2): δ = 7.55 (*ddd*, J = 7.5, 1.4, 0.7 Hz, 4H), 7.46–7.39 (*m*, 4H), 7.35–7.18 (*m*, 8H), 7.13 (*q*, J = 1.0 Hz, 4H), 2.54 (*dd*, J = 5.6, 5.0 Hz, 4H).

^{13}C NMR (75 MHz, CD_2Cl_2): δ = 158.17, 154.26 (*dd*, *J* = 11.0, 8.9 Hz), 128.29 (*t*, *J* = 3.2 Hz), 125.68, 123.29, 121.64, 117.50 (*t*, *J* = 15.5 Hz), 111.75, 21.43 (*dd*, *J* = 6.4, 5.0 Hz).

^{13}C-DEPT-135 NMR (75 MHz, CD_2Cl_2): δ = 125.12 (CH, pos.), 122.73 (CH, pos.), 121.08 (CH, pos.), 116.94 (CH, pos.), 111.19 (CH, pos.), 20.77 (CH_2, neg.).

^{31}P NMR (122 MHz, CD_2Cl_2): δ = −52.60.

HRMS (ESI): *m*/*z* calculated for $C_{34}H_{24}O_4P_2$: 558.1150 $[M+H]^+$, found: 559.1219.

Refinement

Crystal data, data collection and structure refinement details are summarized in Table 1.

References

Ahrens, S., Kusy, R., Spannenberg, A., Vuong, T. H., Rabeah, J., Russbueldt, B. M. E., Panten, J., Jiao, H., Junge, K. & Beller, M. (2025). *J. Am. Chem. Soc.* **147**, 31859–31870.

Benny, A., Sharma, D., Ankur, Rajeshkumar, T., Maron, L. & Venugopal, A. (2023). *Chem. Eur. J.* **29**, e202300588.

Bruker (2013). *SAINT*. Bruker AXS Inc., Madison, Wisconsin, USA.

Bruker (2014). *APEX2*. Bruker AXS Inc., Madison, Wisconsin, USA.

Casey, C. P., Bullock, R. M. & Nief, F. (1983). *J. Am. Chem. Soc.* **105**, 7574–7580.

Clevenger, A. L., Stolley, R. M., Aderibigbe, J. & Louie, J. (2020). *Chem. Rev.* **120**, 6124–6196.

Dekker, G. P. C. M., Elsevier, C. J., Vrieze, K. & Van Leeuwen, P. W. N. M. (1992). *Organometallics* **11**, 1598–1603.

Krause, L., Herbst-Irmer, R., Sheldrick, G. M. & Stalke, D. (2015). *J. Appl. Cryst.* **48**, 3–10.

Leeuwen, P. W. N. M. van, Kamer, P. C. J., Reek, J. N. H. & Dierkes, P. (2000). *Chem. Rev.* **100**, 2741–2770.

Sheldrick, G. M. (2008). *Acta Cryst.* A**64**, 112–122.

Sheldrick, G. M. (2015*a*). *Acta Cryst.* A**71**, 3–8.

Sheldrick, G. M. (2015*b*). *Acta Cryst.* C**71**, 3–8.

Souza, E. L. S., Ahrens, S., Spannenberg, A., Neumann, H., Junge, K., Correia, C. R. D., Jackstell, R. & Beller, M. (2025). *Chem. Commun.* **61**, 9083–9086.

Westrip, S. P. (2010). *J. Appl. Cryst.* **43**, 920–925.

full crystallographic data

IUCrData (2025). **10**, x250916 [https://doi.org/10.1107/S2414314625009162]

1,2-Bis[di(benzofuran-2-yl)phosphanyl]ethane

Sebastian Ahrens, Anke Spannenberg, Matthias Beller and Kathrin Junge

1,2-Bis[di(benzofuran-2-yl)phosphanyl]ethane

Crystal data

$C_{34}H_{24}O_4P_2$
M_r = 558.47
Monoclinic, $P2_1/n$
a = 5.6351 (5) Å
b = 10.5372 (9) Å
c = 22.7988 (19) Å
β = 93.696 (1)°
V = 1350.9 (2) Å^3
Z = 2
$F(000)$ = 580
D_x = 1.373 Mg m^{-3}
Mo $K\alpha$ radiation, λ = 0.71073 Å
Cell parameters from 9822 reflections
θ = 2.6–29.2°
μ = 0.20 mm^{-1}
T = 150 K
Needle, colorless
0.35 × 0.17 × 0.11 mm

Data collection

Bruker APEXII CCD diffractometer
Radiation source: fine-focus sealed tube
Detector resolution: 8.3333 pixels mm^{-1}
φ and ω scans
Absorption correction: multi-scan (SADABS; Krause et al., 2015)
T_{min} = 0.93, T_{max} = 0.98
23407 measured reflections
3594 independent reflections
3145 reflections with $I > 2\sigma(I)$
R_{int} = 0.025
θ_{max} = 29.0°, θ_{min} = 1.8°
h = −7→7
k = −14→14
l = −31→31

Refinement

Refinement on F^2
Least-squares matrix: full
$R[F^2 > 2\sigma(F^2)]$ = 0.038
$wR(F^2)$ = 0.102
S = 1.04
3594 reflections
181 parameters
0 restraints
Hydrogen site location: inferred from neighbouring sites
H-atom parameters constrained
$w = 1/[\sigma^2(F_o^2) + (0.0496P)^2 + 0.6701P]$ where $P = (F_o^2 + 2F_c^2)/3$
$(\Delta/\sigma)_{max}$ = 0.001
$\Delta\rho_{max}$ = 0.41 e Å^{-3}
$\Delta\rho_{min}$ = −0.28 e Å^{-3}

Special details

Geometry. All esds (except the esd in the dihedral angle between two l.s. planes) are estimated using the full covariance matrix. The cell esds are taken into account individually in the estimation of esds in distances, angles and torsion angles; correlations between esds in cell parameters are only used when they are defined by crystal symmetry. An approximate (isotropic) treatment of cell esds is used for estimating esds involving l.s. planes.

Fractional atomic coordinates and isotropic or equivalent isotropic displacement parameters (Å²)

	x	*y*	*z*	U_{iso}*/U_{eq}
P1	0.71188 (6)	0.84518 (3)	0.46075 (2)	0.02309 (10)
O1	0.49580 (18)	0.91096 (10)	0.35215 (4)	0.0306 (2)
O2	0.66914 (17)	0.61479 (9)	0.40832 (4)	0.0265 (2)
C1	0.4685 (2)	0.92984 (11)	0.49513 (6)	0.0236 (2)
H1A	0.320524	0.923062	0.469453	0.028*
H1B	0.439854	0.889731	0.533297	0.028*
C2	0.6973 (3)	0.92132 (12)	0.38979 (6)	0.0275 (3)
C3	0.8541 (3)	1.00332 (13)	0.36809 (6)	0.0280 (3)
H3	1.005756	1.025137	0.385828	0.034*
C4	0.7503 (3)	1.05138 (13)	0.31355 (6)	0.0273 (3)
C5	0.8159 (3)	1.14240 (15)	0.27287 (7)	0.0362 (3)
H5	0.963404	1.185957	0.277924	0.043*
C6	0.6589 (4)	1.16671 (17)	0.22517 (7)	0.0458 (4)
H6	0.698030	1.229013	0.197263	0.055*
C7	0.4426 (4)	1.1010 (2)	0.21721 (7)	0.0491 (4)
H7	0.339642	1.118676	0.183556	0.059*
C8	0.3754 (3)	1.01094 (17)	0.25715 (8)	0.0422 (4)
H8	0.229594	0.965882	0.251760	0.051*
C9	0.5312 (3)	0.99049 (13)	0.30494 (6)	0.0282 (3)
C10	0.5509 (2)	0.70025 (12)	0.44235 (5)	0.0227 (2)
C11	0.3408 (2)	0.65268 (12)	0.45784 (6)	0.0239 (3)
H11	0.229288	0.693672	0.480968	0.029*
C12	0.3194 (2)	0.52756 (12)	0.43237 (5)	0.0231 (2)
C13	0.1490 (3)	0.43112 (13)	0.43126 (6)	0.0284 (3)
H13	0.008549	0.439902	0.451813	0.034*
C14	0.1906 (3)	0.32213 (13)	0.39931 (7)	0.0326 (3)
H14	0.077800	0.255057	0.398549	0.039*
C15	0.3946 (3)	0.30903 (14)	0.36829 (7)	0.0347 (3)
H15	0.416334	0.233660	0.346410	0.042*
C16	0.5668 (3)	0.40349 (14)	0.36860 (7)	0.0327 (3)
H16	0.705679	0.395315	0.347393	0.039*
C17	0.5236 (2)	0.51025 (12)	0.40171 (6)	0.0245 (3)

Atomic displacement parameters (Å²)

	U^{11}	U^{22}	U^{33}	U^{12}	U^{13}	U^{23}
P1	0.02388 (17)	0.01797 (16)	0.02763 (18)	−0.00108 (11)	0.00324 (12)	−0.00143 (11)
O1	0.0314 (5)	0.0278 (5)	0.0333 (5)	−0.0038 (4)	0.0058 (4)	0.0004 (4)
O2	0.0255 (5)	0.0207 (4)	0.0339 (5)	0.0000 (4)	0.0059 (4)	−0.0060 (4)
C1	0.0272 (6)	0.0181 (5)	0.0259 (6)	−0.0009 (5)	0.0047 (5)	−0.0026 (5)
C2	0.0349 (7)	0.0203 (6)	0.0281 (6)	−0.0004 (5)	0.0073 (5)	−0.0034 (5)
C3	0.0339 (7)	0.0230 (6)	0.0273 (6)	−0.0057 (5)	0.0037 (5)	−0.0013 (5)
C4	0.0327 (7)	0.0240 (6)	0.0259 (6)	−0.0005 (5)	0.0072 (5)	−0.0028 (5)
C5	0.0399 (8)	0.0335 (8)	0.0367 (8)	−0.0043 (6)	0.0135 (6)	0.0027 (6)
C6	0.0671 (12)	0.0451 (9)	0.0267 (7)	0.0055 (8)	0.0143 (7)	0.0072 (7)

C7	0.0620 (12)	0.0565 (11)	0.0275 (7)	0.0084 (9)	−0.0089 (7)	−0.0055 (7)
C8	0.0405 (9)	0.0430 (9)	0.0419 (8)	−0.0020 (7)	−0.0059 (7)	−0.0096 (7)
C9	0.0317 (7)	0.0240 (6)	0.0296 (6)	−0.0012 (5)	0.0086 (5)	−0.0043 (5)
C10	0.0263 (6)	0.0172 (5)	0.0247 (6)	0.0020 (4)	0.0028 (5)	−0.0010 (4)
C11	0.0268 (6)	0.0186 (5)	0.0266 (6)	0.0008 (5)	0.0046 (5)	−0.0012 (4)
C12	0.0268 (6)	0.0188 (5)	0.0234 (6)	0.0015 (5)	−0.0017 (5)	0.0010 (4)
C13	0.0296 (7)	0.0239 (6)	0.0315 (7)	−0.0030 (5)	0.0006 (5)	0.0016 (5)
C14	0.0357 (7)	0.0211 (6)	0.0397 (8)	−0.0050 (5)	−0.0074 (6)	−0.0011 (5)
C15	0.0374 (8)	0.0231 (6)	0.0422 (8)	0.0044 (6)	−0.0077 (6)	−0.0110 (6)
C16	0.0299 (7)	0.0284 (7)	0.0396 (8)	0.0051 (5)	0.0003 (6)	−0.0103 (6)
C17	0.0248 (6)	0.0196 (6)	0.0288 (6)	0.0012 (5)	−0.0014 (5)	−0.0017 (5)

Geometric parameters (Å, º)

P1—C2	1.8028 (14)	C6—H6	0.9500
P1—C10	1.8117 (13)	C7—C8	1.384 (3)
P1—C1	1.8519 (13)	C7—H7	0.9500
O1—C2	1.3829 (18)	C8—C9	1.371 (2)
O1—C9	1.3887 (17)	C8—H8	0.9500
O2—C17	1.3758 (15)	C10—C11	1.3531 (18)
O2—C10	1.3869 (15)	C11—C12	1.4425 (17)
C1—C1^{i}	1.533 (2)	C11—H11	0.9500
C1—H1A	0.9900	C12—C17	1.3965 (19)
C1—H1B	0.9900	C12—C13	1.3971 (18)
C2—C3	1.3520 (19)	C13—C14	1.388 (2)
C3—C4	1.4321 (19)	C13—H13	0.9500
C3—H3	0.9500	C14—C15	1.394 (2)
C4—C9	1.394 (2)	C14—H14	0.9500
C4—C5	1.400 (2)	C15—C16	1.390 (2)
C5—C6	1.381 (2)	C15—H15	0.9500
C5—H5	0.9500	C16—C17	1.3850 (18)
C6—C7	1.404 (3)	C16—H16	0.9500
C2—P1—C10	100.04 (6)	C9—C8—H8	121.9
C2—P1—C1	99.98 (6)	C7—C8—H8	121.9
C10—P1—C1	97.50 (6)	C8—C9—O1	126.45 (14)
C2—O1—C9	106.27 (11)	C8—C9—C4	123.73 (14)
C17—O2—C10	106.06 (10)	O1—C9—C4	109.80 (12)
C1^{i}—C1—P1	110.79 (12)	C11—C10—O2	111.43 (11)
C1^{i}—C1—H1A	109.5	C11—C10—P1	133.26 (10)
P1—C1—H1A	109.5	O2—C10—P1	115.17 (9)
C1^{i}—C1—H1B	109.5	C10—C11—C12	106.59 (11)
P1—C1—H1B	109.5	C10—C11—H11	126.7
H1A—C1—H1B	108.1	C12—C11—H11	126.7
C3—C2—O1	110.67 (12)	C17—C12—C13	118.91 (12)
C3—C2—P1	128.31 (11)	C17—C12—C11	105.69 (11)
O1—C2—P1	120.64 (10)	C13—C12—C11	135.38 (13)
C2—C3—C4	107.70 (13)	C14—C13—C12	118.18 (14)

C2—C3—H3	126.1	C14—C13—H13	120.9
C4—C3—H3	126.1	C12—C13—H13	120.9
C9—C4—C5	119.42 (14)	C13—C14—C15	121.37 (13)
C9—C4—C3	105.53 (12)	C13—C14—H14	119.3
C5—C4—C3	134.98 (14)	C15—C14—H14	119.3
C6—C5—C4	117.75 (15)	C16—C15—C14	121.64 (13)
C6—C5—H5	121.1	C16—C15—H15	119.2
C4—C5—H5	121.1	C14—C15—H15	119.2
C5—C6—C7	121.14 (16)	C17—C16—C15	115.93 (14)
C5—C6—H6	119.4	C17—C16—H16	122.0
C7—C6—H6	119.4	C15—C16—H16	122.0
C8—C7—C6	121.67 (16)	O2—C17—C16	125.85 (13)
C8—C7—H7	119.2	O2—C17—C12	110.19 (11)
C6—C7—H7	119.2	C16—C17—C12	123.94 (13)
C9—C8—C7	116.23 (16)		

C2—P1—C1—C1^{i}	−66.72 (13)	C3—C4—C9—O1	1.48 (15)
C10—P1—C1—C1^{i}	−168.36 (12)	C17—O2—C10—C11	0.95 (14)
C9—O1—C2—C3	0.12 (15)	C17—O2—C10—P1	177.25 (9)
C9—O1—C2—P1	173.64 (9)	C2—P1—C10—C11	−113.82 (14)
C10—P1—C2—C3	−150.90 (13)	C1—P1—C10—C11	−12.23 (15)
C1—P1—C2—C3	109.56 (13)	C2—P1—C10—O2	70.91 (10)
C10—P1—C2—O1	36.84 (11)	C1—P1—C10—O2	172.49 (9)
C1—P1—C2—O1	−62.70 (11)	O2—C10—C11—C12	0.06 (15)
O1—C2—C3—C4	0.80 (16)	P1—C10—C11—C12	−175.35 (10)
P1—C2—C3—C4	−172.09 (10)	C10—C11—C12—C17	−1.02 (14)
C2—C3—C4—C9	−1.38 (15)	C10—C11—C12—C13	−179.30 (14)
C2—C3—C4—C5	175.51 (16)	C17—C12—C13—C14	−0.27 (19)
C9—C4—C5—C6	−0.7 (2)	C11—C12—C13—C14	177.84 (14)
C3—C4—C5—C6	−177.27 (16)	C12—C13—C14—C15	−0.9 (2)
C4—C5—C6—C7	−1.0 (2)	C13—C14—C15—C16	0.9 (2)
C5—C6—C7—C8	1.2 (3)	C14—C15—C16—C17	0.3 (2)
C6—C7—C8—C9	0.4 (3)	C10—O2—C17—C16	177.01 (13)
C7—C8—C9—O1	175.93 (14)	C10—O2—C17—C12	−1.61 (14)
C7—C8—C9—C4	−2.2 (2)	C15—C16—C17—O2	179.94 (13)
C2—O1—C9—C8	−179.39 (15)	C15—C16—C17—C12	−1.6 (2)
C2—O1—C9—C4	−1.02 (14)	C13—C12—C17—O2	−179.74 (11)
C5—C4—C9—C8	2.4 (2)	C11—C12—C17—O2	1.64 (14)
C3—C4—C9—C8	179.90 (14)	C13—C12—C17—C16	1.6 (2)
C5—C4—C9—O1	−176.00 (12)	C11—C12—C17—C16	−177.01 (13)

Symmetry code: (i) −*x*+1, −*y*+2, −*z*+1.